Hindawi
Advances in Civil Engineering
Volume 2021, Article ID 5549891, 16 pages
https://doi.org/10.1155/2021/5549891

Research Article

Establishment of Rutting Model of Wheel-Tracking Test for Real-Time Prediction of Rut Depth of Asphalt Layers

Yulong Zhao,[1,2] **Ying Gao**,[2] **Ke Zhang**,[3] **Yao Zhang**,[4] **and Mingce Yu**[5]

[1]*School of Civil Engineering, Shandong Jiaotong University, Jinan 250357, China*
[2]*School of Transportation, Southeast University, Nanjing 211189, China*
[3]*College of Information Engineering, Fuyang Normal University, Fuyang 236041, China*
[4]*College of Civil Science and Engineering, Yangzhou University, Yangzhou 225127, China*
[5]*School of Highway and Architecture, Shandong Transport Vocational College, Weifang 261206, China*

Correspondence should be addressed to Ying Gao; gy@seu.edu.cn

Received 9 March 2021; Revised 27 May 2021; Accepted 8 June 2021; Published 21 June 2021

Academic Editor: Valeria Vignali

The construction process control of asphalt layers directly affects the road service life and quality. The objective of this study was to establish a rutting model of the wheel-tracking test used for the real-time prediction of the rut depth of asphalt layers in the construction process. The gradation of asphalt mixture, asphalt content, and molding temperature were considered in the development of the new rutting model of the wheel-tracking test. The effects of these three factors on the high-temperature performance of asphalt mixture were analyzed. The order of importance of the factors affecting the high-temperature performance of asphalt mixture is the gradation of asphalt mixture, asphalt-aggregate ratio, and molding temperature. Overall, the predicted values of the rut depth of the wheel-tracking test are very close to the measured values. Furthermore, the difference between the rut depths of asphalt layers of the test group and the control group is small. These comparison results indicate that the new rutting model of the wheel-tracking test has high accuracy and good applicability for the test road.

1. Introduction

Rutting is one of the main early distresses in asphalt pavements, which not only significantly reduces the service quality and service life of the road but also poses a serious threat to the driving of the vehicle [1–3]. Through investigation, it was found that bad construction quality of the asphalt layer is one of the main reasons for the early distresses in asphalt pavement [4, 5]. The construction indices are commonly used to control the construction quality of the asphalt layer [6, 7], such as asphalt-aggregate ratio, gradation of asphalt mixture, and rolling temperature. However, the development of rutting is not given in the construction process of the asphalt layer, which is not conducive to reducing the early distresses in asphalt pavements. Furthermore, when the construction factors affecting the asphalt pavement performance are in an unfavourable situation, although they meet the requirements of the construction specification, the asphalt pavement performance may not meet the expected requirements. Consequently, in the construction process of the asphalt layer, it is important to predict the rut depth of asphalt pavement in real time to control the construction quality of the asphalt layer.

A variety of rutting models have been established to estimate the development of the rut depth of asphalt pavement. The resilient strain of the asphalt layer, the number of load repetitions, and the temperature were used to predict the asphalt pavement rutting in the MEPDG design method [8]. The distinguishing feature of this model was the consideration of the mechanical response of the pavement structure and the asphalt mixture performance. The format of the NCHRP 1-40B rutting model [9] is the same as that of the MEPDG rutting model. The difference between these two models is that the material properties and volumetric properties of the asphalt mixture are adopted to adjust the permanent deformation constants for the NCHRP 1-40B rutting model. The NCHRP 9-25 rutting model is based on the material properties, voids in the mineral

aggregate, and compaction parameters to estimate the rutting rate [10]. Le et al. [11] proposed a rutting model for South Korean Pavement Design Guide, and the model variables are the number of loadings, temperature, and initial air voids. The rutting model proposed by Kim et al. [12] is based on the number of loads, the loading time, temperature, and the ratio of shear stress to shear strength. In China, the JTG D50-2017 rutting model is used to verify the alternative pavement structure in the design phase of road projects [13]. The model variables mainly include the permanent deformation equivalent temperature of the asphalt layer, the rut depth of the wheel-tracking test, and the number of load repetitions. Wang et al. [14] established a rutting model for the Asphalt Pavement Analyzer rutting test. The variables mainly include temperature, loading time, loading level, and air void.

To predict the rut depth of asphalt pavement in real time during construction, an accurate rutting model needs to be selected. When determining the rutting model, two principles should be considered: (1) the rutting model should have high accuracy for road construction projects; (2) the model variables can be detected or predicted in the construction process of the asphalt layer. The accuracy of the rutting models is best compared by the long-term follow-up monitoring of the actual road rut, but there are currently no corresponding complete test data. Each rutting model is based on a certain foundation, which is inseparable from the materials, pavement design, and construction methods of the corresponding countries. Therefore, the applicability of the foreign rutting model in China needs further verification. In China, the pavement structure is designed according to JTG D50-2017 [13]. Its design requirements can be used for construction process control. Furthermore, the JTG D50-2017 rutting model [13] had been verified by the actual road projects of China. Therefore, the JTG D50-2017 rutting model [13] was selected for real-time prediction of the permanent deformation of asphalt layers.

The JTG D50-2017 rutting model [13] needs to input the permanent deformation of the wheel-tracking test. This model variable cannot be detected in real time during the actual construction of the asphalt layer. It is necessary to estimate the rut depth of the wheel-tracking test according to the real-time detection data of the asphalt layer. Therefore, the model for rut depth of the wheel-tracking test should be proposed as the submodel of the JTG D50-2017 rutting model [13].

According to the NCHRP 704 report [15] and the findings by Rahman [16], the main factors affecting the high-temperature performance of asphalt pavement are the gradation of asphalt mixture, the properties of the asphalt, the effective asphalt content, the air voids, and the thicknesses of the asphalt layers. In the asphalt mixture plant, the gradation of the asphalt mixture can be predicted in real time by the digital image processing technology [17–20] or online detection [6, 7]. The asphalt-aggregate ratio can be detected in real time by the online detection of the asphalt mixture plant [6]. The ground-penetrating radar can be used to estimate the air voids and the thicknesses of the asphalt layers in real time [21–24]. Based on the air voids and the related information of aggregates, the effective asphalt content can be calculated [6].

This paper aims to propose a rutting model of the wheel-tracking test for monitoring the construction quality of the asphalt layer in real time. The model variables can be determined in real time during the construction of the asphalt layer. The wheel-tracking test was conducted according to T 0719-2011 of JTG E20-2011 [25]. The rutting model of the wheel-tracking test was verified by road test results. The JTG D50-2017 rutting model [13] was used to predict the rutting development of the pavement structure. Furthermore, the effect of the deviation of the rutting model of the wheel-tracking test on the rut depth of pavement structure was analyzed.

2. Experimental Program

2.1. Raw Materials. Two types of asphalt mixtures, AC-13 and SUP-20, were used for the wheel-tracking test.

2.1.1. Asphalt Binder. The SBS-modified asphalt (I-C) was selected for AC-13. Its properties are shown in Table 1. The requirements for the material properties of asphalt were according to JTG F40-2004 [6]. The tests shown in Table 1 were conducted based on JTG E20-2011 [25]. Table 2 presents the properties of asphalt for SUP-20, which was SBS-modified asphalt with the performance grade of PG 76-22.

2.1.2. Mineral Aggregate. The sizes of the aggregates used for AC-13 were 0~2.36 mm, 2.36~4.75 mm, 4.75~9.5 mm, and 9.5~13.2 mm. The properties of these aggregates are shown in Table 3. The tests shown in Table 3 are carried out in accordance with JTG E42-2005 [31]. Five different sizes of aggregates were used for SUP-20, which were 0~2.36 mm, 2.36~4.75 mm, 4.75~9.5 mm, 9.5~13.2 mm, and 13.2~19 mm. Table 4 lists the properties of the aggregates for SUP-20. The mineral powder is limestone flour. According to JTG F40-2004 [6], the mineral powder for the asphalt mixture must be ground from hydrophobic stone such as limestone or strong basic rock in magmatic rock, and the soil impurities in the original stone should be removed.

2.2. Design of Mix Proportion. The designed gradations of AC-13 and SUP-20 are shown in Figure 1. For AC-13 and SUP-20, the optimum asphalt-aggregate ratios (OARs), which were 5.0% and 4.5%, were determined based on the Marshall design method and Superpave design method, respectively. The molding temperature of specimens was 160°C, which was related to the initial rolling temperature. The design results for the asphalt mixtures of AC-13 and SUP-20 are shown in Table 5. According to the location of the road construction project, the design results met the technical requirements of JTG F40-2004 [6] and AASHTO M 323 [35], respectively.

2.3. Variability Design of Construction Control Indices. According to the requirements of construction specifications of asphalt pavements [6, 7], the influencing factors of

Table 1: Properties of asphalt for AC-13.

Item		Tested result	Requirement	Test method [25]
Penetration (25°C, 100 g, 5 s) (0.1 mm)		68	60 ~ 80	T 0604
Penetration index		0.32	≥ −0.4	T 0604
Ductility (5°C, 5 cm/min) (cm)		44	≥ 30	T 0605
Softening point (°C)		77.9	≥ 55	T 0606
Kinematical viscosity (135°C) (Pa s)		1.73	≤ 3	T 0625
Flashpoint (°C)		256	≥ 230	T 0611
Solubility in trichloroethylene (%)		99.64	≥ 99	T 0607
Elastic recovery (%)		85.8	≥ 65	T 0662
Density (25°C) (g/cm^3)		1.023	NA	T 0603
Storage stability (°C)		1.3	≤ 2.5	T 0661
Thin-film oven test (163°C)	Mass loss (%)	−0.04919	−1.0 ~ 1.0	T 0609
	Residual penetration ratio (25°C) (%)	73.5	≥ 60	T 0604
	Residual ductility (5°C) (cm)	26.37	≥ 20	T 0605

Table 2: Properties of asphalt for SUP-20.

		Item		Tested result	Requirement	Test method
Original asphalt	—	135°C	Kinematical viscosity (Pa s)	2.500	≤3	AASHTO T 316 [26]
	DSR	76°C	G* (kPa)	1.52	G*·sinδ ≥1.0	AASHTO T 315 [27]
			δ	69.2		
			G*·sinδ (kPa)	1.63		
	DSR	82°C	G* (kPa)	0.869		
			δ	67.7		
			G*·sinδ (kPa)	0.939		
RTFOT	DSR	76°C	G* (kPa)	2.58	G*·sinδ ≥2.2	AASHTO T 240 [28]
			δ	66.2		
			G*·sinδ	2.82		
	DSR	82°C	G* (kPa)	1.52		AASHTO T 315 [27]
			δ	68.2		
			G*·sinδ (kPa)	1.64		
PAV	BBR	−12°C	S (MPa)	145	S ≤300	AASHTO R 28 [29]
			m		m ≥0.300	
		−18°C	S (MPa)	268		AASHTO T 313 [30]
			m	0.284		
	DSR	31°C	G* (kPa)	1010	G*·sinδ ≤5000	AASHTO R 28 [29]
			δ	64.4		
			G*·sinδ (kPa)	910.9		AASHTO T 315 [27]

Note. RTFOT: Rolling Thin-Film Oven Test. PAV: Pressurized Aging Vessel. DSR: Dynamic Shear Rheometer. BBR: Bending Beam Rheometer. G* denotes the complex shear modulus. δ denotes the phase angle.

Table 3: Properties of aggregates for AC-13.

Item			Test result	Requirement	Test method
Coarse aggregate		Crushing value (%)	16.9	≤26	T0316
		Loss by abrasion and impact of the sample (%)	17.5	≤28	T0317
	9.5~13.2 mm	Percentage of flat-elongated particles (%)	6.9	≤12	T0312
	4.75~9.5 mm		6.3	≤18	
		Polished stone value	46	≥42	T0321
Fine aggregate		Sand equivalent (%)	68	≥60	T 0334
		Solidness (%)	16	≥12	T 0340

Table 4: Properties of aggregates for SUP-20.

Item	Test result	Requirement	Test method
Angularity of coarse aggregate	100	≥85/80	ASTM D5821 [32]
Angularity of fine aggregate	46.6	≥45	AASHTO T304 [33]
Percentage of flat-elongated particles (%)	7.3	≤15	T 0312 JTG E20-2011 [25]
Sand equivalent (%)	68	≥45	AASHTO T 176 [34]

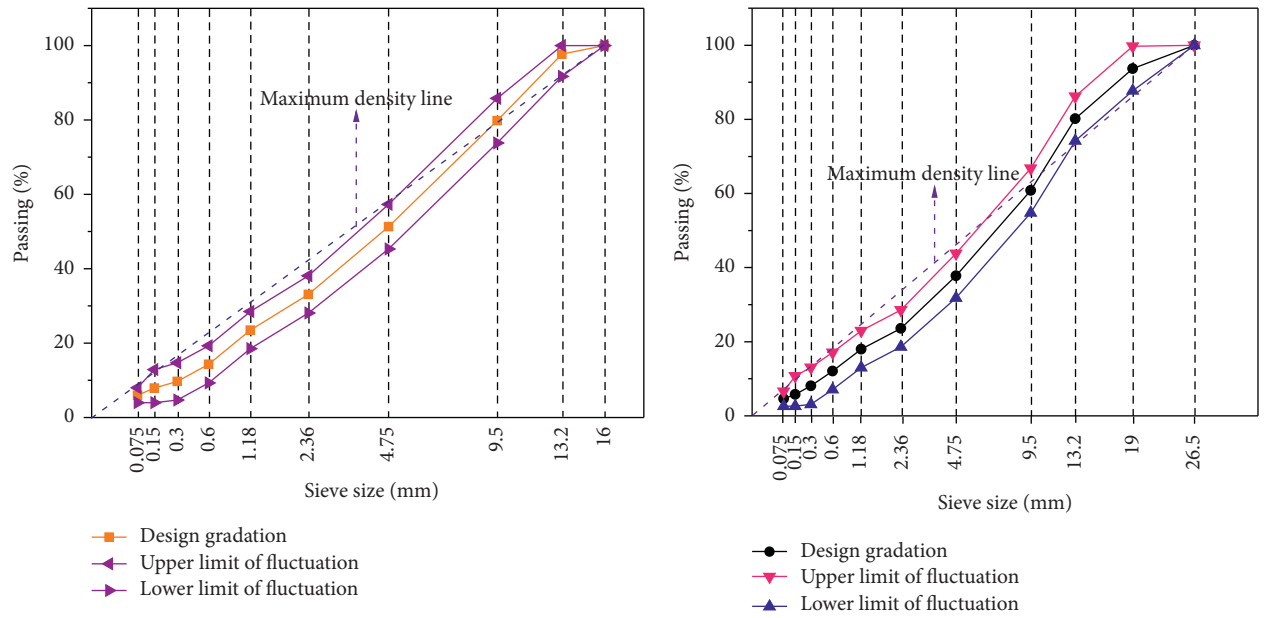

Figure 1: Design gradations of (a) AC-13 and (b) SUP-20.

Table 5: Properties of the asphalt mixtures based on the OARs.

Type	OARs (%)	Air voids (%)	Voids filled with asphalt (%)	Voids in mineral aggregate (%)	Marshall stability (kN)	Marshall flow (0.1 mm)
AC-13	5.0	3.8	72.8	14.0	11.17	26.9
SUP-20	4.5	4.0	69.3	13.0	—	—

the construction quality of asphalt layers mainly include raw material quality, mineral gradation, asphalt content, construction temperature, rolling passes, degree of compaction, thickness of the asphalt layer, and evenness. By analyzing these factors, it can be found that, for the construction process of the asphalt layer, the main factors affecting the construction quality can be essentially summarized as mineral gradation, asphalt content, rolling temperature, rolling passes, and thickness of the compacted asphalt layer. With the widespread use of Global Positioning System-Real-Time Kinematic (GPS-RTK) technology, the number of rolling passes is well controlled [36]. RTK is a real-time dynamic relative positioning technology using GPS carrier phase observations; the working principle of RTK is that the base station transmits its observations and station coordinate information to the mobile station through the data link. Therefore, the main considered factors of construction quality were mineral gradation, asphalt content, and rolling temperature in this study, which can be determined in real time. In the asphalt mixture plant, the allowable fluctuation ranges of mineral gradation for the AC-13 and SUP-20 are shown in Figures 1(a) and 1(b), respectively [6, 37]. The asphalt content should be controlled at the range of design value ±0.3% [6]. In this research, the degree of fluctuation in the molding temperature was designed to be ±15°C.

The aggregate segregation and temperature differential can occur in the production, transportation, and paving processes of asphalt mixture. Previous studies have shown that aggregate segregation and temperature differential have adverse effects on the asphalt pavement performance [38–42]. Therefore, the influence of segregation on the high-temperature performance of asphalt mixture was considered for establishing a more suitable rutting model of the wheel-tracking test. In the actual construction process, aggregate segregation is very complex. In this study, the degree of segregation aggregate is mainly characterized by the percent passing of 2.36 mm sieve, which is the key sieve. The contained aggregates in the asphalt mixture are divided into two parts by the 2.36 mm sieve. Part 1 was composed of particles passing through the 2.36 mm sieve. The particles retained on the 2.36 mm sieve composed part 2. The following method was used to simulate the aggregate segregation of asphalt mixture: increasing (decreasing) the mass of each size of particles of P1 part in equal proportion and decreasing (increasing) the mass of each size of particles of P2 part correspondingly. Four different levels of aggregate segregation for AC-13 were designed in this study, which are shown in Figure 2. For the temperature differential, the set molding temperatures were 145°C and 130°C. The air voids of asphalt mixtures with different degrees of segregation were determined by the means of the Superpave gyratory

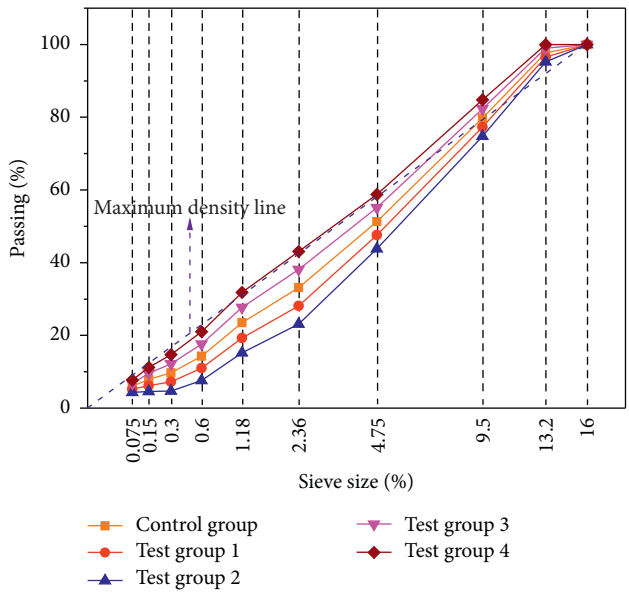

Figure 2: Designed aggregate segregation for AC-13.

compactor, and the effect of nonsegregation area on the segregation area was considered in this study [43]. Further information related to the determination of air voids can be found in [43]. The test conditions of different groups of asphalt mixtures are shown in Table 6.

2.4. Specimen Preparation and Testing Procedures. The specimen preparation was conducted according to T 0703-2011 of JTG E20-2011 [25]. The size of the slab specimen for the wheel-tracking test is 300 mm (long) × 300 mm (wide) × 50 mm (height). First, the mesh mold was put into an oven at a temperature of 100°C for one hour. Then, the mesh mold was taken out of the oven. A plain paper was laid in the mesh mold. Next, the asphalt mixture was mixed again by a spatula. The asphalt mixture was placed evenly in the mesh mold from side to center, and the middle part of the paved asphalt mixture was slightly higher than the surrounding area. The frame was removed, and a preheated compact hammer was used to tamp the paved asphalt mixture from the edge to the middle, as shown in Figure 3. When the asphalt mixture reached the molding temperature, a plain paper was placed on the surface of the asphalt mixture. Then, the mesh mold containing the asphalt mixture was put on the platform of the roller compactor. The total load used for compaction was adjusted to 9 kN. In general, the set air voids can be achieved by 24 passes according to the T 0703-2011 of JTG E20-2011 [25].

The wheel-tracking test was required by the JTG D50-2017 rutting model of the asphalt pavement, which was performed in accordance with T 0719-2011 of JTG E20-2011 [25], as shown in Figure 4. The test temperature was 60°C, and the wheel pressure was 0.7 MPa. The slab specimen together with the mesh mold was placed in an incubator with a temperature of 60 ± 1°C for 5 hours. Then, the slab specimen together with the mesh mold was placed on the test platform of the rutting test machine. The wheel reciprocates over the specimen with a travel distance of 230 ± 10 mm. The frequency of the wheel ranges from 42 ± 1 passes per minute across the specimen. The rutting test machine was started to make the test wheel travel back and forth. The rut depth was collected by the rut deformation automatic recorder.

2.5. JTG D50-2017 Rutting Model of Asphalt Pavement. According to JTG D50-2017 [13], the rut depth of asphalt layers can be predicted using the following equations:

$$\begin{aligned} R_a &= \sum_{i=1}^{n} R_{ai}, \\ R_{ai} &= 2.31 \times 10^{-8} k_{Ri} T_{pef}^{2.93} p_i^{1.80} N_{e3}^{0.48} (h_i/h_0) R_{0i}, \\ k_{Ri} &= (d_1 + d_2 z_i) \cdot 0.9731^{z_i}, \\ d_1 &= -1.35 \times 10^{-4} h_a^2 + 8.18 \times 10^{-2} h_a - 14.50, \\ d_2 &= 8.78 \times 10^{-7} h_a^2 - 1.50 \times 10^{-3} h_a + 0.90, \end{aligned} \quad (1)$$

where R_a is the rut depth of the asphalt layers (mm); R_{ai} is the rut depth of sublayer i (mm); n is the number of sublayers; T_{pef} is the equivalent temperature for the permanent deformation of the asphalt layer (°C); N_{e3} is the number of equivalent load repetitions on the design lane; h_i is the thickness of sublayer i (mm); h_0 is the thickness of the slab specimen for the wheel-tracking test (mm); R_{0i} is the permanent deformation of wheel-tracking test for the asphalt mixture of sublayer i when the number of wheel passes is 2520 (mm); k_{Ri} is the comprehensive correction coefficient; z_i is the depth of sublayer i (mm); h_a is the total asphalt layers thickness (mm); p_i is the vertical compressive stress of the top surface of sublayer i (MPa).

3. Results and Discussion

3.1. Results of Wheel-Tracking Test. Table 7 presents the results of the wheel-tracking test.

3.1.1. Effect of Gradation on Rut Depth of Wheel-Tracking Test. Based on Tables 6 and 7, the influence of gradation level on rut depth of wheel-tracking test is shown in Figure 5. For the design gradation of AC-13, the rut depth is 2.603 mm, which is the average value of the rut depths of groups 10~18. From Figure 5, it can be observed that, for the set gradation levels, the rut depth increases as the gradation level changes from the upper limit of fluctuation through the design gradation to the lower limit of fluctuation. This is because the asphalt content is at a high level for the three gradation levels. When the gradation level changes from fine gradation to coarse gradation, the specific surface area of the mineral material decreases. Therefore, the free asphalt increases, which leads to the increase of the rut depth. Furthermore, when the gradation changes from the design level to the lower limit of the gradation fluctuation, the asphalt mixture becomes difficult to be compacted, causing a decrease in the high-temperature performance of the asphalt mixture.

Table 6: Test conditions of different groups of asphalt mixtures.

Group		Gradation	Asphalt content (%)	Molding temperature (°C)	Air voids (%)
1	AC-13	Upper limit of fluctuation	4.5	145	1
2	AC-13	Upper limit of fluctuation	4.5	160	2
3	AC-13	Upper limit of fluctuation	4.5	175	3
4	AC-13	Upper limit of fluctuation	4.8	145	4
5	AC-13	Upper limit of fluctuation	4.8	160	5
6	AC-13	Upper limit of fluctuation	4.8	175	6
7	AC-13	Upper limit of fluctuation	5.0	145	7
8	AC-13	Upper limit of fluctuation	5.0	160	8
9	AC-13	Upper limit of fluctuation	5.0	175	9
10	AC-13	Design gradation	4.5	145	10
11	AC-13	Design gradation	4.5	160	11
12	AC-13	Design gradation	4.5	175	12
13	AC-13	Design gradation	4.8	145	13
14	AC-13	Design gradation	4.8	160	14
15	AC-13	Design gradation	4.8	175	15
16	AC-13	Design gradation	5.0	145	16
17	AC-13	Design gradation	5.0	160	17
18	AC-13	Design gradation	5.0	175	18
19	AC-13	Lower limit of fluctuation	4.5	145	19
20	AC-13	Lower limit of fluctuation	4.5	160	20
21	AC-13	Lower limit of fluctuation	4.5	175	21
22	AC-13	Lower limit of fluctuation	4.8	145	22
23	AC-13	Lower limit of fluctuation	4.8	160	23
24	AC-13	Lower limit of fluctuation	4.8	175	24
25	AC-13	Lower limit of fluctuation	5.0	145	25
26	AC-13	Lower limit of fluctuation	5.0	160	26
27	AC-13	Lower limit of fluctuation	5.0	175	27
28	AC-13	Aggregate segregation 1	4.1	160	28
29	AC-13	Aggregate segregation 2	3.5	160	29
30	AC-13	Aggregate segregation 3	5.5	160	30
31	AC-13	Aggregate segregation 4	6.2	160	31
32	AC-13	Design gradation	4.8	130	32
33	SUP-20	Upper limit of fluctuation	4.0	145	33
34	SUP-20	Upper limit of fluctuation	4.0	160	34
35	SUP-20	Upper limit of fluctuation	4.0	175	35
36	SUP-20	Upper limit of fluctuation	4.3	145	36
37	SUP-20	Upper limit of fluctuation	4.3	160	37
38	SUP-20	Upper limit of fluctuation	4.3	175	38
39	SUP-20	Upper limit of fluctuation	4.6	145	39
40	SUP-20	Upper limit of fluctuation	4.6	160	40
41	SUP-20	Upper limit of fluctuation	4.6	175	41
42	SUP-20	Design gradation	4.0	145	42
43	SUP-20	Design gradation	4.0	160	43
44	SUP-20	Design gradation	4.0	175	44
45	SUP-20	Design gradation	4.3	145	45
46	SUP-20	Design gradation	4.3	160	46
47	SUP-20	Design gradation	4.3	175	47
48	SUP-20	Design gradation	4.6	145	48
49	SUP-20	Design gradation	4.6	160	49
50	SUP-20	Design gradation	4.6	175	50
51	SUP-20	Lower limit of fluctuation	4.0	145	51
52	SUP-20	Lower limit of fluctuation	4.0	160	52
53	SUP-20	Lower limit of fluctuation	4.0	175	53
54	SUP-20	Lower limit of fluctuation	4.3	145	54
55	SUP-20	Lower limit of fluctuation	4.3	160	55
56	SUP-20	Lower limit of fluctuation	4.3	175	56
57	SUP-20	Lower limit of fluctuation	4.6	145	57
58	SUP-20	Lower limit of fluctuation	4.6	160	58
59	SUP-20	Lower limit of fluctuation	4.6	175	59
60	SUP-20	Design gradation	4.3	130	60

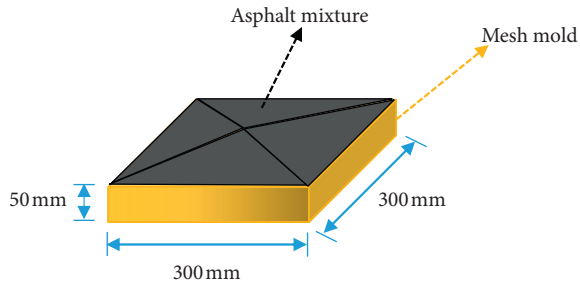

Figure 3: Manufacturing process of the slab specimen.

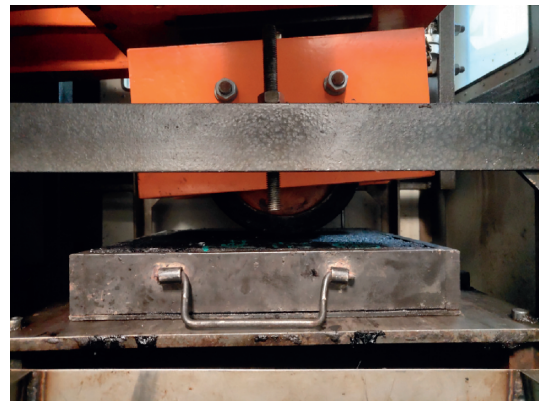

Figure 4: Wheel-tracking test apparatus.

Table 7: Results of the wheel-tracking test.

Group	RD (mm)	Group	RD (mm)	Group	RD (mm)	Group	RD (mm)
1	2.086	16	3.822	31	6.474	46	1.635
2	1.961	17	3.915	32	2.996	47	1.352
3	1.490	18	4.451	33	2.193	48	2.965
4	1.585	19	3.955	34	2.155	49	3.223
5	1.479	20	3.823	35	2.126	50	3.368
6	1.657	21	3.011	36	2.068	51	2.985
7	3.263	22	4.141	37	1.936	52	2.726
8	3.966	23	4.960	38	1.919	53	2.667
9	4.449	24	5.319	39	1.862	54	3.418
10	2.398	25	5.689	40	1.711	55	3.227
11	1.729	26	5.920	41	2.131	56	2.982
12	1.315	27	6.968	42	1.758	57	4.710
13	2.563	28	1.467	43	1.669	58	4.409
14	1.601	29	2.485	44	1.522	59	4.653
15	1.636	30	6.044	45	1.703	60	1.796

Note. RD is the rut depth.

3.1.2. Effect of Asphalt Content on Rut Depth of Wheel-Tracking Test. Figure 6 presents the relationship between the asphalt content and the rut depth of the wheel-tracking test according to Tables 6 and 7. For 4.8% of the asphalt content of AC-13, the rut depth is 2.771 mm, which is the average value of the rut depths of groups 4, 5, 6, 13, 14, 15, 22, 23, and 24. For the set asphalt content, the curve of the rut depth is relatively flat when the asphalt content ranges from 4.5% (4.0%) to 4.8% (4.3%). The rut depth of the wheel-tracking test increases as the asphalt content increases from 4.8% (4.3%) to 5.0% (4.6%). As the asphalt content increases, the free asphalt in the asphalt mixture increases, which leads to a decrease in the high-temperature stability of the asphalt mixture.

3.1.3. Effect of Molding Temperature on Rut Depth of Wheel-Tracking Test. Figure 7 shows the effect of molding temperature on the rut depth of the wheel-tracking test on the basis of Tables 6 and 7. For 160°C of the molding temperature of AC-13, the rut depth of the wheel-tracking test is 3.262 mm, which is the average value of the rut depths of groups 2, 5, 8, 11, 14, 17, 20, 23, and 26. When the molding temperature raises from 145°C to 160°C, the rut depth of the

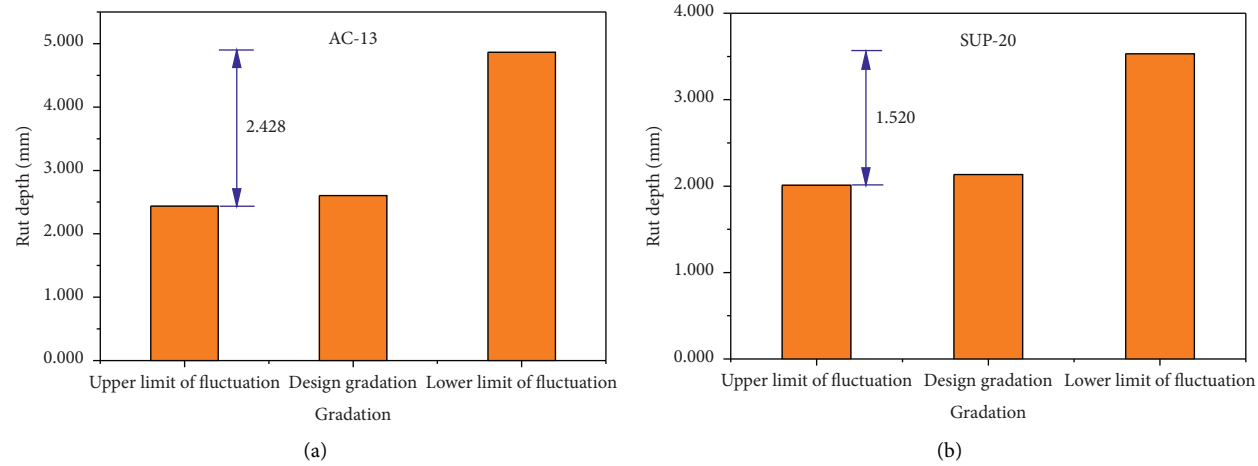

Figure 5: Variation in rut depth with gradation.

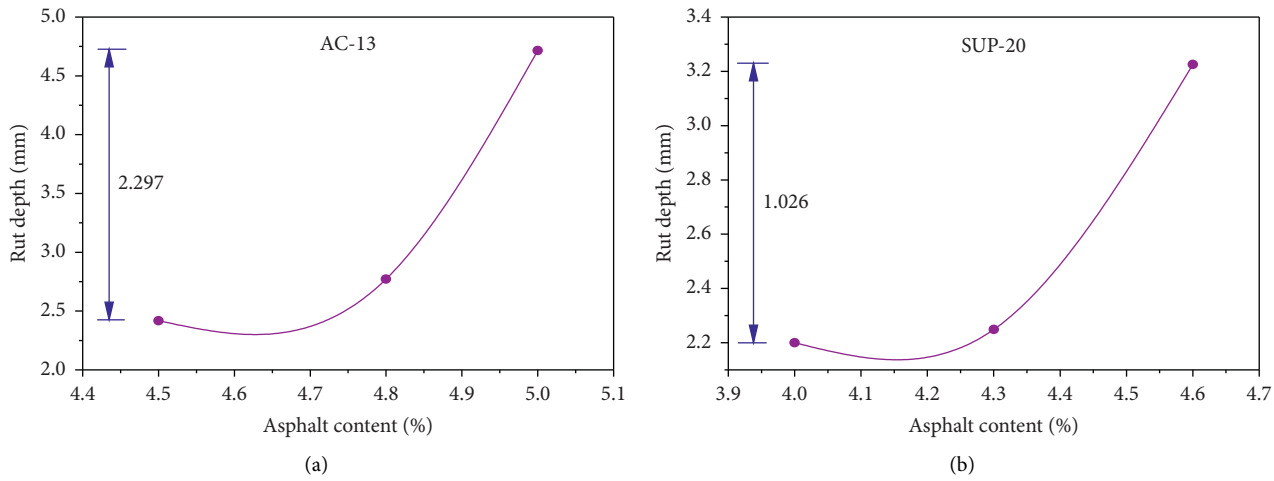

Figure 6: Variation in rut depth with asphalt content.

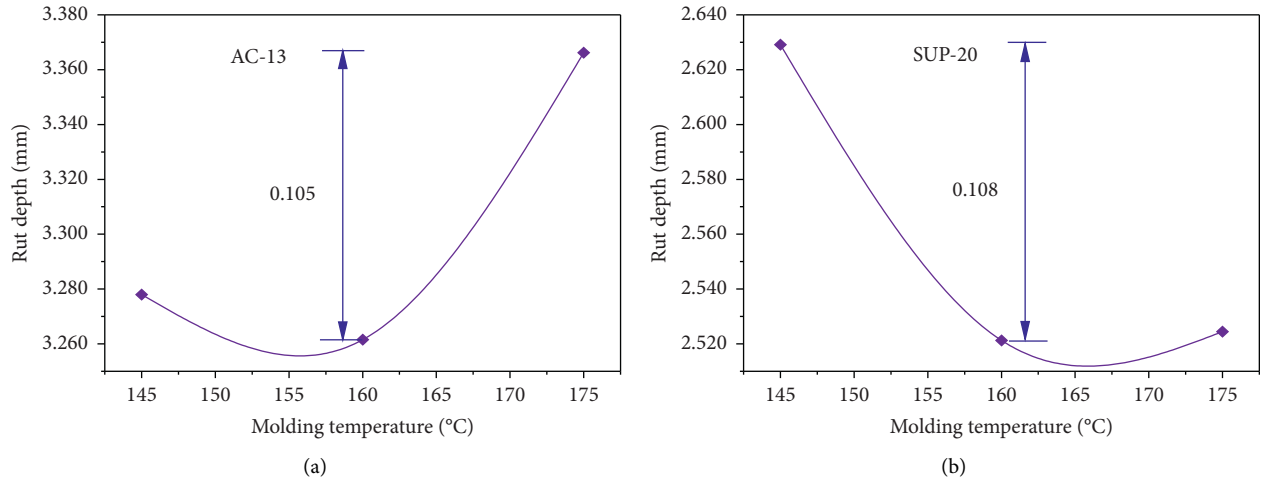

Figure 7: Variation in rut depth with molding temperature.

wheel-tracking test decreases. This is mainly because the asphalt consistency is reduced, the asphalt film thickness increases, and the mixture becomes easy to be compacted. However, the rut depth of the wheel-tracking test increases as the molding temperature ranges from 160°C to 175°C. This can be attributed to the decrease of air voids, the decrease of the asphalt film thickness, and the increase of free asphalt.

On the other hand, the importance of each factor can be evaluated according to Figures 5–7. For the given factor levels, the order of factors is gradation, asphalt content, and molding temperature in accordance with the influence degree of factors from strong to weak.

3.2. Rutting Model of Wheel-Tracking Test. According to NCHRP 704 report [15] and Rahman et al. [44], the main factors affecting the permanent deformation of the asphalt layer are cumulative percent retained on the 3/4 inch, 3/8 inch, no. 4 standard sieves, percent passing of no. 200 standard sieves, the properties of asphalt, effective asphalt content, air voids, effective binder content, and the thickness of the asphalt layer. For the properties of asphalt, Rahman et al. [44] mainly used two viscosity-temperature susceptibility parameters A and VTS to predict the rutting depth of the Hamburg Wheel-Tracking Device test. In this study, the established rutting model of the wheel-tracking test will be used to evaluate the high-temperature performance of the asphalt layer in real time. Unfortunately, the properties of asphalt and the thickness of the asphalt layer are not easy to be detected in real time. The air voids of the asphalt layer can be estimated according to the findings by Zhao [43] or measured by the intelligent roller [45]. Then, the effective binder content can be calculated based on JTG F40-2004 [6]. The gradation of asphalt mixture can be in real time obtained from the asphalt mixture plant. This paper mainly considers the effects of gradation, effective asphalt content, and air voids on the permanent deformation of the asphalt mixture. The data used to establish the rutting model of the wheel-tracking test are shown in Table 8.

According to the above analysis of the factors affecting the asphalt pavement rutting, a new rutting model of the wheel-tracking test was established based on the data shown in Table 8. Data fitting was carried out in a nonlinear way. The new rutting model was mainly in the form of polynomials.

$$\begin{aligned}\lg(RD) = {} & -2.393 + 8.186\lg(P_{38}) - 2.934\left[\lg(P_{38})\right]^2 - 1.733\lg(P_4) \\ & + 0.793\left[\lg(P_4)\right]^2 - 3.929\lg(P_{200}) + 2.611\left[\lg(P_{200})\right]^2 - 5\lg\left(V_{beff}\right) \\ & + 4.754\left[\lg\left(V_{beff}\right)^2\right] - 1.935\lg(V_a) + 1.855\left[\left[\lg(V_a)\right]^2 R^2 = 0.724.\right.\end{aligned} \tag{2}$$

Based on Table 8, the estimated values of the rut depth of wheel-tracking test are shown in Figure 8, compared with the measured values. Different from the previous rut prediction model of the wheel-tracking test [44], this model can predict the rut depth of the compacted asphalt mixture in real time.

3.3. Verification of Rutting Model of Wheel-Tracking Test. After the rutting model of the wheel-tracking test is established, it needs to be verified based on road construction projects. Figure 9 and Table 9 present the gradations and asphalt contents of the asphalt mixture sampled from a highway construction project in Jiangsu province of China by the extraction tests (ETs), respectively. The asphalt mixture was prepared according to the results of the ETs. The molding temperature is shown in Table 10, which is measured by the infrared temperature sensors. Based on the air voids of the asphalt mixture determined by the Superpave gyratory compactor, the slab specimens were molded, and the rut depths of these specimens were obtained using the wheel-tracking test. For the extraction test groups, the predicted and measured values of the rut depth of the wheel-tracking test are shown in Figure 10.

The applicability of the rutting model of the wheel-tracking test was evaluated by using the deviation between the estimated and the measured values of each extraction test group. According to Figure 10, the average deviation between the predicted and the measured values of rut depths of the extraction groups is 6.62%. The maximum deviation of these extraction test groups is 19.19%. Except for the 8th extraction group, the absolute values of the deviations of the other extraction groups were less than 14%. Overall, the deviation between the predicted and measured values of the rut depths of these extraction test groups is relatively small, indicating that the rutting model of the wheel-tracking test established in this study has good applicability for the test road.

3.4. Effect of Deviation of Rutting Model of Wheel-Tracking Test on Prediction Accuracy of JTG D50-2017 Rutting Model of Asphalt Layers. The influence of the difference between the estimated and measured values of rut depths of wheel-tracking test on the rut depths of asphalt layers predicted by the JTG D50-2017 rutting model [13] was investigated in this study.

3.4.1. Asphalt Pavement Structure and Traffic Parameters. The pavement structure was mainly determined based on the design data of the highway construction project and JTG D50-2017 [13], which is shown in Figure 11. The traffic volume of large passenger cars and trucks on the highway section was set at 4,750 vehicles per day, with an annual growth rate of 5%.

Table 8: Data summary for the establishment of the permanent deformation prediction model of the wheel-tracking test.

Group	P_{38} (%)	P_4 (%)	P_{200} (%)	V_{beff} (%)	V_a (%)	RD (mm)
1	14.2	42.7	8	9.45	5.0	2.086
2	14.2	42.7	8	9.49	4.6	1.961
3	14.2	42.7	8	9.51	4.4	1.490
4	14.2	42.7	8	10.15	4.3	1.585
5	14.2	42.7	8	10.20	3.8	1.479
6	14.2	42.7	8	10.21	3.7	1.657
7	14.2	42.7	8	10.83	3.7	3.263
8	14.2	42.7	8	10.90	3.1	3.966
9	14.2	42.7	8	10.92	2.9	4.449
10	20.2	48.7	6	9.43	4.8	2.398
11	20.2	48.7	6	9.47	4.4	1.729
12	20.2	48.7	6	9.49	4.2	1.315
13	20.2	48.7	6	10.14	4.0	2.563
14	20.2	48.7	6	10.17	3.7	1.601
15	20.2	48.7	6	10.19	3.5	1.636
16	20.2	48.7	6	10.87	3.0	3.822
17	20.2	48.7	6	10.90	2.7	3.915
18	20.2	48.7	6	10.92	2.6	4.451
19	26.2	54.7	4	9.17	6.9	3.955
20	26.2	54.7	4	9.21	6.4	3.823
21	26.2	54.7	4	9.25	6.0	3.011
22	26.2	54.7	4	9.90	5.8	4.141
23	26.2	54.7	4	9.93	5.5	4.960
24	26.2	54.7	4	9.96	5.2	5.319
25	26.2	54.7	4	10.59	5.0	5.689
26	26.2	54.7	4	10.66	4.4	5.920
27	26.2	54.7	4	10.68	4.2	6.968
28	22.7	52.4	5.2	8.19	8.7	1.467
29	25.2	56.2	4.3	6.51	10.6	2.485
30	17.7	44.9	6.8	11.81	3.1	6.044
31	15.2	41.2	7.7	13.41	2.5	6.474
32	20.2	48.7	6	10.00	5.3	2.996
33	33.2	56.2	6.6	8.31	5.2	2.193
34	33.2	56.2	6.6	8.32	5.0	2.155
35	33.2	56.2	6.6	8.33	4.9	2.126
36	33.2	56.2	6.6	8.96	4.7	2.068
37	33.2	56.2	6.6	9.00	4.3	1.936
38	33.2	56.2	6.6	9.01	4.2	1.919
39	33.2	56.2	6.6	9.62	4.1	1.862
40	33.2	56.2	6.6	9.67	3.7	1.711
41	33.2	56.2	6.6	9.69	3.5	2.131
42	39.2	62.2	4.6	8.46	5.0	1.758
43	39.2	62.2	4.6	8.47	4.9	1.669
44	39.2	62.2	4.6	8.50	4.6	1.522
45	39.2	62.2	4.6	9.14	4.3	1.703
46	39.2	62.2	4.6	9.16	4.1	1.635
47	39.2	62.2	4.6	9.17	3.9	1.352
48	39.2	62.2	4.6	9.83	3.4	2.965
49	39.2	62.2	4.6	9.87	3.1	3.223
50	39.2	62.2	4.6	9.88	3.0	3.368
51	45.2	68.2	2.6	8.34	6.4	2.985
52	45.2	68.2	2.6	8.39	5.9	2.726
53	45.2	68.2	2.6	8.41	5.6	2.667
54	45.2	68.2	2.6	9.09	4.9	3.418
55	45.2	68.2	2.6	9.11	4.7	3.227
56	45.2	68.2	2.6	9.14	4.4	2.982
57	45.2	68.2	2.6	9.73	4.5	4.710
58	45.2	68.2	2.6	9.77	4.1	4.409
59	45.2	68.2	2.6	9.78	4.0	4.653
60	39.2	62.2	4.6	9.04	5.3	1.796

Note. P_{38} is the cumulative percent retained on a 3/8-inch sieve. P_4 is cumulative percent retained on no. 4 sieve. P_{200} is the percent passing no. 200 sieve. V_{beff} is effective asphalt content. V_a is the air voids of asphalt mixture.

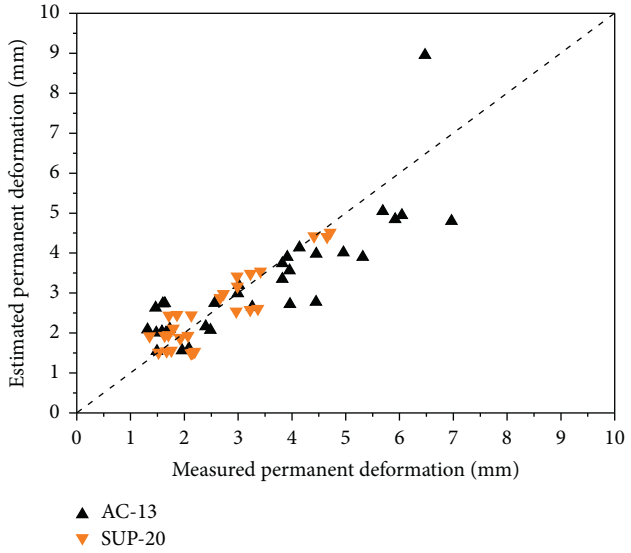

Figure 8: Comparisons of measured and estimated values of rut depth of wheel-tracking test.

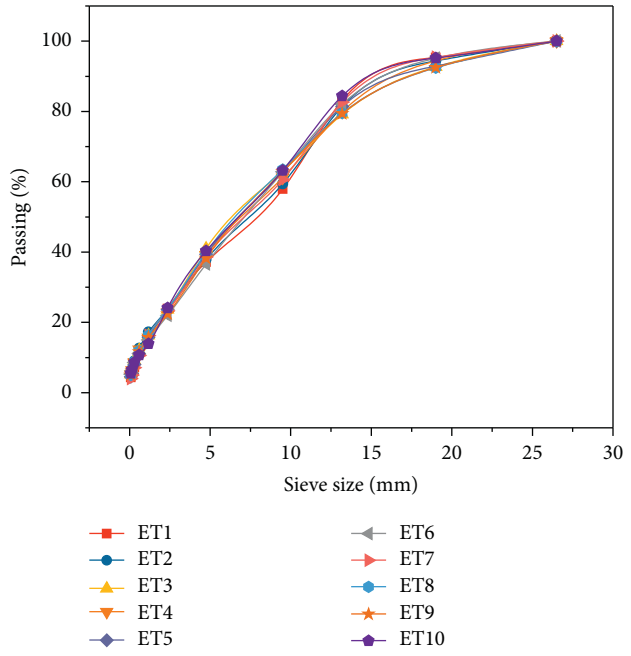

Figure 9: Gradations of the asphalt mixture by the ETs.

Table 9: Asphalt content of the asphalt mixture by the ETs.

Number of the ETs	1	2	3	4	5	6	7	8	9	10
Asphalt content (%)	4.29	4.33	4.32	4.32	4.55	4.34	4.39	4.32	4.30	4.31

Table 10: Molding temperatures for the extraction test groups.

Number of the ETs	1	2	3	4	5	6	7	8	9	10
Molding temperature (°C)	154	161	150	153	155	151	155	152	161	160

The design life of this highway was 15 years. According to the recommended value of JTG D50-2017 [13], the directional distribution factor was set to 0.55, and the lane distribution factor was set to 0.78. The vehicle class distribution factors were determined according to truck traffic classification (TTC) 1 of JTG D50-2017 [13], as shown in Table 11.

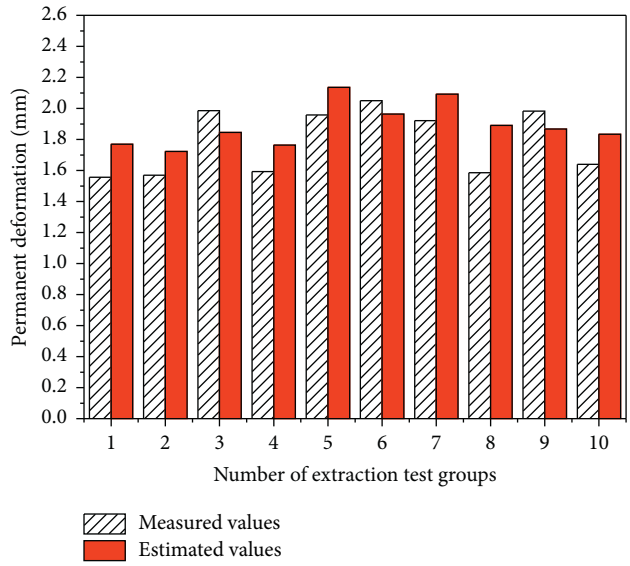

Figure 10: Comparison between the predicted and measured values of the rut depth of the wheel-tracking test.

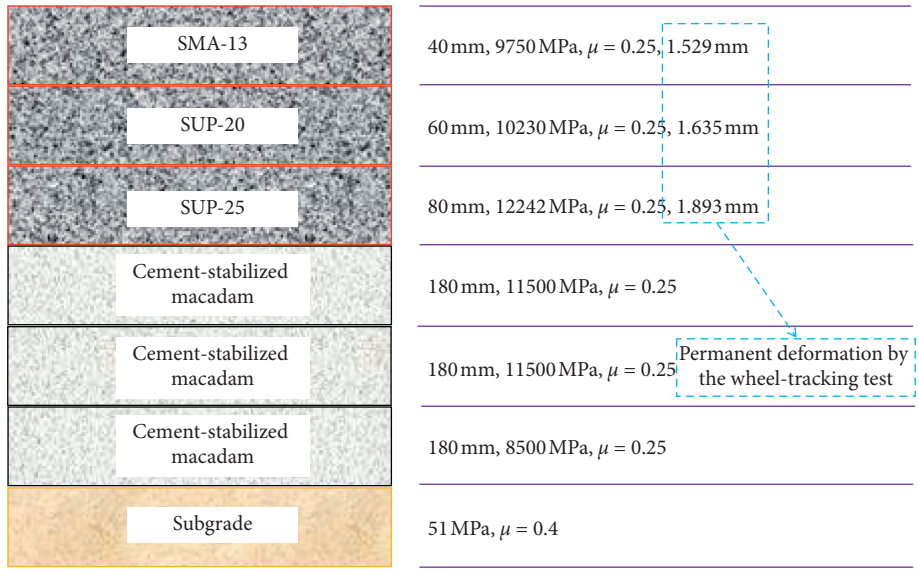

Figure 11: Pavement structure for analysis.

According to JTG D50-2017 [13], the proportion of not fully loaded and fully loaded vehicles of each type is shown in Table 12; the conversion factor of equivalent single axle loads is shown in Table 13. The cumulative equivalent single axle loads can be calculated by [13]

$$N_1 = \mathrm{AADTT} \times \mathrm{DDF} \times \mathrm{LDF} \times \sum_{m=2}^{11} \left(\mathrm{VCDF}_m \times \mathrm{EALF}_m\right),$$

$$N_e = \frac{\left[(1+\gamma)^t - 1\right] \times 365}{\gamma} N_1, \tag{3}$$

where N_1 is the average daily equivalent single axle loads of the design lane; AADTT is the annual average daily truck and large-size passenger bus traffic (vehicle/d); DDF is the directional distribution factor; LDF is the lane distribution factor; m is the vehicle class number; VCDF_m is the distribution factor of vehicle class m; EALF_m is the conversion factor of equivalent single axle loads of vehicle class m; N_e is the cumulative equivalent single axle loads of the design lane in the design service life; t is the design service life of pavement (year); γ is the annual average growth rate of traffic in the design service life.

The influence of the temperature condition at the location of the road project was considered by the JTG D50-2017 rutting model of the asphalt layers [13]. For the city of Nanjing and pavement structure, the equivalent temperature for the permanent deformation of the asphalt layer was 25.0°C, that is, T_{pef} = 25.0°C. According to JTG D50-2017 [13], the asphalt mixture layers shown in Figure 11 were layered, and the thicknesses of these sublayers were 10 mm, 15 mm, 15 mm, 20 mm, 20 mm, 20 mm, and 80 mm. The vertical compressive

Table 11: Vehicle class distribution factors.

TTC group	Vehicle class distribution (%)									
	2	3	4	5	6	7	8	9	10	11
1	6.4	15.3	1.4	0.0	11.9	3.1	16.3	20.4	25.2	0.0

Table 12: Proportion of not fully loaded and fully loaded vehicles.

Vehicle class	Not fully loaded vehicle	Fully loaded vehicles
2	0.85	0.15
3	0.90	0.10
4	0.65	0.35
5	0.75	0.25
6	0.55	0.45
7	0.70	0.30
8	0.45	0.55
9	0.60	0.40
10	0.55	0.45
11	0.65	0.35

Table 13: Conversion factor of equivalent single axle loads.

Vehicle class	Tensile strain at the bottom of asphalt layer and permanent deformation of asphalt layer		Tensile stress at the bottom of inorganic binder stabilized layer	
	Not fully loaded vehicle	Fully loaded vehicle	Not fully loaded vehicle	Fully loaded vehicle
2	0.8	2.8	0.5	35.5
3	0.4	4.1	1.3	314.2
4	0.7	4.2	0.3	137.6
5	0.6	6.3	0.6	72.9
6	1.3	7.9	10.2	1505.7
7	1.4	6.0	7.8	553.0
8	1.4	6.7	16.4	713.5
9	1.5	5.1	0.7	204.3
10	2.4	7.0	37.8	426.8
11	1.5	12.1	2.5	985.4

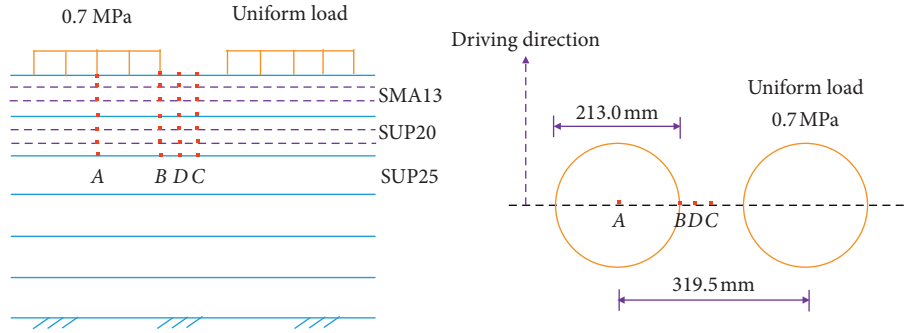

Figure 12: Load parameters and calculation point positions.

stress at the top of each sublayer was calculated using the elastic layer system theory. The load parameters and calculation point positions [13] are shown in Figure 12. By calculation, the rutting of the asphalt layer is 14.9 mm for the design service life, which meets the design requirement of JTG D50-2017 (≤15.0 mm) [13]. The development of rutting with the service life is shown in Figure 13.

3.4.2. Rutting Prediction Results of Asphalt Layers. The cylinder specimens used for the dynamic modulus test were molded according to the air voids of the asphalt mixtures for each extraction test group. The dynamic modulus test was conducted according to T 0738-2011 of JTG E20-2011 [25], and the test conditions were 20°C and 10 Hz. For each extraction test group, the results of the dynamic modulus test are shown in Figure 14. According to the JTG D50-2017 rutting model of the asphalt layers [13], the rutting prediction results of asphalt layers are shown in Figure 15. In this paper, the predicted rut depths of asphalt layers using the measured rut depths of wheel-tracking test are classified as the control group. The rest, which are based on the predicted rut depths of wheel-tracking test, are classified as the test group.

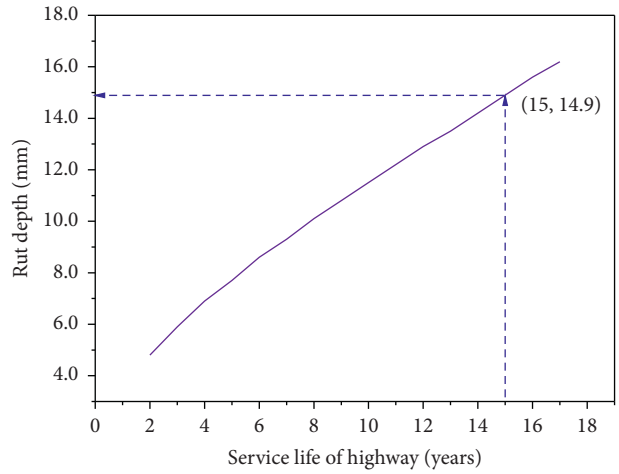

Figure 13: Relationship between the estimated rut depth of highway and service life.

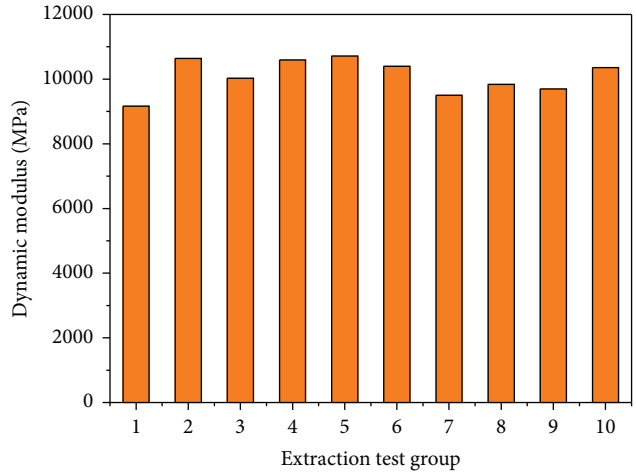

Figure 14: Results of the dynamic modulus test for the extraction test groups.

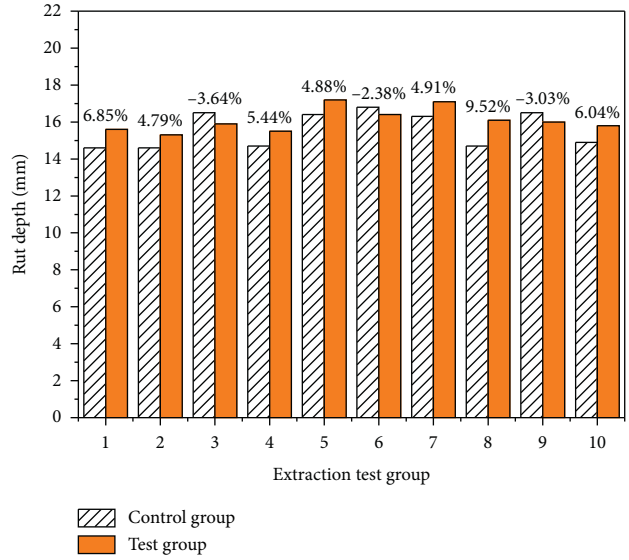

Figure 15: Rutting prediction results of asphalt layers for the extraction test groups.

From Figure 15, the average deviation of the rut depths of the asphalt layers between the control group and the test group is 3.34%. For the extraction test groups 1~10, the largest deviation is 9.52%. Furthermore, the absolute values of the deviations for these extraction test groups are all less than 10%. The results indicated that the influence of the deviation between the predicted and measured values of rut depths of wheel-tracking test on the rutting prediction results of JTG D50-2017 is small.

4. Conclusions

In this study, a new rutting model of the wheel-tracking test was proposed as the submodel of the JTG D50-2017 rutting model of the asphalt layers, which can be used to monitor the construction quality of the asphalt layer in real time. The gradation, asphalt-aggregate ratio, and molding temperature were considered as the factors affecting the permanent deformation of the wheel-tracking test. The new rutting model of the wheel-tracking test was verified based on a road construction project. Furthermore, the effect of using the estimated value of rut depth of wheel-tracking test instead of the measured values was analyzed in this study. Based on the results and analysis, the following conclusions can be drawn:

(1) For the given factor levels, the permanent deformation of the asphalt mixture increases as the gradation level changes from the upper limit of fluctuation through the design gradation to the lower limit of fluctuation. In the asphalt mixture plant, the coarser gradation of asphalt mixture has an adverse influence on the high-temperature of the asphalt mixture if the asphalt content is at a high level.

(2) For the given factor levels, increasing the asphalt content overall leads to the increase of the permanent deformation of the asphalt mixture. There is a suitable molding temperature to obtain better high-temperature performance of asphalt mixture, which is near the designed molding temperature.

(3) For the given factor levels, the influence degree of the three factors on the permanent deformation of the asphalt mixture is in such an order: gradation, asphalt content, and molding temperature.

(4) Based on the results of the extraction test, the deviation between the predicted and measured values of rut depth of wheel-tracking test is small, which indicates that the new rutting model of the wheel-tracking test has good applicability for SUP20.

(5) The deviation between the rut depths of asphalt layers of the test group and the control group is small, which also indicates that the new rutting model of the wheel-tracking test has good prediction accuracy for SUP20.

Data Availability

The data used to support the findings of this study are included within the article.

Conflicts of Interest

The authors declare that there are no conflicts of interest regarding the publication of this paper.

Acknowledgments

This study was supported by the Shandong Provincial Natural Science Foundation (ZR2020QE274), Key Research and Development Program of Shandong Province (Soft Science Project) (2020RKB01602), Science and Technology Plan of Shandong Transportation Department (2019B63 and 2020B93), National Natural Science Foundation of China (51878168), Open Research Fund of National Engineering Laboratory for Advanced Road Materials (NLARM-ORF-2018-01), Provincial Natural Science Foundation of Anhui (1908085QE217), and Key Project of Natural Science Research of Anhui Provincial Department of Education (KJ2018A0668 and KJ2020A1214).

References

[1] X. Zhao, A. Shen, and B. Ma, "Temperature adaptability of asphalt pavement to high temperatures and significant temperature differences," *Advances in Materials Science and Engineering*, vol. 2018, Article ID 9436321, 16 pages, 2018.

[2] X. Dai, Y. Jia, S. Wang, and Y. Gao, "Evaluation of the rutting performance of the field specimen using the Hamburg wheel-tracking test and dynamic modulus test," *Advances in Civil Engineering*, vol. 2020, Article ID 9525179, 15 pages, 2020.

[3] T. Chopra, M. Parida, N. Kwatra, and P. Chopra, "Development of pavement distress deterioration prediction models for urban road network using genetic programming," *Advances in Civil Engineering*, vol. 2018, Article ID 1253108, 15 pages, 2018.

[4] A. E. Abu El-Maaty, A. Y. Akal, and S. El-Hamrawy, "Management of highway projects in Egypt through identifying factors influencing quality performance," *Journal of Construction Engineering*, vol. 2016, Article ID 4823630, 8 pages, 2016.

[5] J. Shen, F. Li, and J. Chen, *Analysis and Preventiue Techniques of Premature Damage of Asphalt Pavement in Expressway*, China Communications Press, Beijing, China, 2004.

[6] J.TGF40-2004, *Technical Specifications for Construction of Highway Asphalt Pavements*, China Communications Press, Beijing, China, 2004.

[7] North Carolina Department of Transportation, *Hot Mix Asphalt Quality Management System*, North Carolina Department of Transportation, Raleigh, NC, USA, 2012.

[8] A. Inc, *Guide for Mechanistic–Empirical Design of New and Rehabilitated Pavement Structures*, National Cooperative Highway Research Program, Washington, DC, USA, 2004.

[9] F. Zhou, E. Fernando, and T. Scullion, *A Review of Performance Models and Test Procedures with Recommendations for Use in the Texas Me Design Program*, Texas Transportation Institute, Bryan, TX, USA, 2008.

[10] D. W. Christensen and R. F. Bonaquist, *Volumetric Requirements for Superpave Mix Design*, Transportation Research Board, Washington, DC, USA, 2006.

[11] A. T. Le, H. J. Lee, H. M. Park, and S. Y. Lee, "Development of a permanent deformation model of asphalt mixtures for South Korean pavement design guide," *Transportation Research Record*, vol. 2095, no. 1, pp. 45–52, 2009.

[12] W. J. Kim, V. P. Le, H. J. Lee, and H. T. Phan, "Calibration and validation of a rutting model based on shear stress to strength ratio for asphalt pavements," *Construction and Building Materials*, vol. 149, pp. 327–337, 2017.

[13] JTG D50-2017, *Specifications for Design of Highway Asphalt Pavement*, China Communications Press, Beijing, China, 2017.

[14] H. Wang, H. Tan, T. Qu et al., "Effects of test conditions on APA rutting and prediction modeling for asphalt mixtures," *Advances in Materials Science and Engineering*, vol. 2017, Article ID 2062758, 11 pages, 2017.

[15] I. N. Fugro Consultants and S. Arizona, *A Performance-Related Specification for Hot-Mixed Asphalt*, Transportation Research Board, Washington, DC, USA, 2011.

[16] A. A. Rahman, M. M. Mendez Larrain, and R. A. Tarefder, "Development of a nonlinear rutting model for asphalt concrete based on weibull parameters," *International Journal of Pavement Engineering*, vol. 20, no. 6, pp. 1–10, 2017.

[17] T. Wang, *Research of Intelligent Technology of Quality Process Control of Asphalt Pavement*, Hebei University of Technology, Tianjin, China, 2014.

[18] P. Zou, *The Design and Implementation of Real-Time Detection System for Aggregate Gradation Based on Multi-Source Vision*, Chang'an University, Xi'an, China, 2015.

[19] I. S. Bessa, V. T. F. Castelo Branco, and J. B. Soares, "Evaluation of different digital image processing software for aggregates and hot mix asphalt characterizations," *Construction and Building Materials*, vol. 37, pp. 370–378, 2012.

[20] M. Moaveni, *Advanced Image Analysis and Techniques for Degradation Characterization of Aggregates*, University of Illinois at Urbana-Champaign, Champaign, IL, USA, 2015.

[21] P. Shangguan, I. L. Al-Qadi, Z. Leng, R. L. Schmitt, and A. Faheem, "Innovative approach for asphalt pavement compaction monitoring with ground-penetrating radar," *Transportation Research Record*, vol. 2347, no. 1, pp. 79–87, 2013.

[22] E. Kassem, A. Chowdhury, T. Scullion, and E. Masad, "Application of ground-penetrating radar in measuring the density of asphalt pavements and its relationship to mechanical properties," *International Journal of Pavement Engineering*, vol. 17, no. 6, pp. 503–516, 2016.

[23] I. L. Al-Qadi, S. Lahouar, and A. Loulizi, "Successful application of ground-penetrating radar for quality assurance-quality control of new pavements," *Transportation Research Record*, vol. 1861, no. 1, pp. 86–97, 2003.

[24] S. Zhao, P. Shangguan, and I. L. Al-Qadi, "Application of regularized deconvolution technique for predicting pavement thin layer thicknesses from ground penetrating radar data," *NDT & E International*, vol. 73, pp. 1–7, 2015.

[25] JTGE20-2011, *Standard Test Methods of Bitumen and Bituminous Mixtures for Highway Engineering*, China Communications Press, Beijing, China, 2011.

[26] T. Aashto, *Standard Method of Test for Viscosity Determination of Asphalt Binder using Rotational Viscometer*, American Association of State Highway and Transportation Officials, Washington, DC, USA, 2017.

[27] T. Aashto, *Standard Method of Test for Determining the Rheological Properties of Asphalt Binder using a Dynamic Shear Rheometer (DSR)*, American Association of State Highway and Transportation Officials, Washington, DC, USA, 2016.

[28] T. Aashto, *Standard Method of Test for Effect of Heat and Air on a Moving Film of Asphalt Binder (Rolling Thin-Film Oven Test)*, American Association of State Highway and Transportation Officials, Washington, DC, USA, 2017.

[29] R. Aashto, *Standard Practice for Accelerated Aging of Asphalt Binder Using a Pressurized Aging Vessel (PAV)*, American Association of State Highway and Transportation Officials, Washington, DC, USA., 2016.

[30] T. Aashto, *Standard Method of Test for Determining the Flexural Creep Stiffness of Asphalt Binder Using the Bending Beam Rheometer (BBR)*, American Association of State Highway and Transportation Officials, Washington, DC, USA, 2016.

[31] JTGE42-2005, *Test Methods of Aggregate for Highway Engineering*, China Communications Press, Beijing, China, 2005.

[32] ASTM D5821, *Standard Test Method for Determining the Percentage of Fractured Particles in Coarse Aggregate*, ASTM International, West Conshohocken, PA, USA, 2017.

[33] T. Aashto, *Standard Method of Test for Uncompacted Void Content of Fine Aggregate*, American Association of State Highway and Transportation Officials, Washington, DC, USA, 2017.

[34] T. Aashto, *Standard Method of Test For Plastic Fines in Graded Aggregates and Soils by Use of the Sand Equivalent Test*, American Association of State Highway and Transportation Officials, Washington, DC, USA, 2017.

[35] M. Aashto, *Standard Specification for Superpave Volumetric Mix Design*, American Association of State Highway and Transportation Officials, Washington, DC, USA, 2017.

[36] L. Zhang, *Research on Information-Based Control of Asphalt Pavement Compaction*, Southeast University, Nanjing, China, 2014.

[37] DB32/T1246, *Standard Specification for Construction of Jiangsu Province Expressway Asphalt Pavements*, Nanjing, China, 2008.

[38] K. A. Willoughby, J. S. Uhlmeyer, J. P. Mahoney et al., "Construction-related variability in pavement mat density due to temperature differentials," *Transportation Research Record*, vol. 1849, no. 1, pp. 166–173, 2003.

[39] A. Shen, Y. Guo, F. Che et al., "Influence of asphalt mixture segregation on long-term high temperature performance of asphalt pavement based on MMLS3 test," *China Journal Of Highway And Transport*, vol. 25, no. 3, pp. 80–86, 2012.

[40] M. Stroup-Gardiner and E. R. Brown, *Segregation in Hot-Mix Asphalt Pavements*, Transportation Research Board, Washington, DC, USA, 2000.

[41] W. Wu, Z. Tu, Z. Zhu et al., "Effect of gradation segregation on mechanical properties of an asphalt mixture," *Applied Sciences*, vol. 9, no. 2, pp. 1–15, 2019.

[42] L. Garcia-Gil, R. Miró, and F. E. Pérez-Jiménez, "Evaluating the role of aggregate gradation on cracking performance of asphalt concrete for thin overlays," *Applied Sciences*, vol. 9, no. 4, pp. 1–17, 2019.

[43] Y. Zhao, *Research on Construction Process Control of Asphalt Layer Based on BIM Technology*, Southeast University, Nanjing, China, 2018.

[44] A. A. Rahman, M. M. Mendez Larrain, and R. A. Tarefder, "Development of a nonlinear rutting model for asphalt concrete based on weibull parameters," *International Journal of Pavement Engineering*, vol. 20, no. 9, pp. 1055–1064, 2019.

[45] Q. Xu, G. K. Chang, and V. Gallivan, "A sensing-information-statistics integrated model to predict asphalt material density with intelligent compaction system," *IEEE*, vol. 20, no. 6, pp. 3204–3211, 2015.